ELSEVIER

PII: S0032-3861(97)00122-5

Polymer Vol. 38 No. 23, pp. 5801–5806, 1997

0032-3861/97/$17.00+0.00

Thermally stimulated modulus relaxation in polymers: method and interpretation

Hermann Wagner and Ranko Richert*
Max-Planck-Institut für Polymerforschung, Ackermannweg 10, 55128 Mainz, Germany
(Received 12 June 1996; revised 1 January 1997)

We have measured the thermally stimulated decay of the dielectric modulus $M(T, t)$ for poly(vinylacetate) by monitoring the electric field $E(t)$ under the condition of a constant dielectric displacement for $t > 0$. This thermally stimulated polarization experiment is realized by cooling the sample at zero field to well below its glass transition temperature, applying a certain amount of charge, and then recording the voltage of the sample capacitor $U(T, t)$ while ramping the temperature. The result of a temperature invariant distribution of relaxation times observed previously in isothermal experiments allows a direct translation of $M(T, t)$ data into the variation of a characteristic relaxation time $\tau(T)$ or of a fictive temperature $T_f(T)$ as a function of the actual temperature. © 1997 Elsevier Science Ltd.

(Keywords: thermally stimulated discharge; dielectric relaxation and retardation; glass transition)

INTRODUCTION

The majority of applications of polymers relies on the common experience that these disordered materials solidify at sufficiently low temperatures below the glass transition temperature T_g so that the desired mechanical stability is achieved[1]. Applications which critically demand a static matrix are polymer-based nonlinear optical devices where molecular mobility will counteract the alignment of the oriented hyperpolarizable species, thereby restoring the centrosymmetry of the sample and degrading the second harmonic generation efficiency[2,3]. The transition from the liquid state above T_g to the glassy frozen state below T_g is a kinetic phenomenon, indicating only that the system is no longer capable of attaining the thermodynamic equilibrium within a certain time scale defined by experimental conditions[4]. The experimental signature of the kinetic nature of T_g is its dependence on the cooling or heating rate or on the longest time scale accessible in an isothermal experiment. For instance, a carefully cooled sample can still display the behaviour of an equilibrium liquid at dielectric relaxation times as high as 10^7 s without interfering with the glass transition[5]. Less precise but more practical ways of outlining T_g are for instance features in differential scanning calorimetry (d.s.c.) traces at a specified heating rate (denoted T_g^* in the following), a viscosity linked definition in terms of $\eta(T_g) = 10^{13}$ Poise, or a dielectric relaxation time $\tau(T_g) = 100\,s$[6].

Above T_g polymers usually display dispersive, i.e. non-exponential, relaxation patterns $\phi(t)$ which are well described by the stretched exponential or Kohlrausch–Williams–Watts[7,8] (KWW) function

$$\phi(t) = \phi_0 \exp[-(t/\tau_{KWW})^{\beta_{KWW}}] \quad (1)$$

In this KWW expression τ_{KWW} is a characteristic relaxation time and β_{KWW} within the limits $0 < \beta_{KWW} < 1$ quantifies the extent of deviation from a single exponential decay with $\beta_{KWW} = 1$ or equivalently the degree of the relaxation time dispersion. In case the distribution of relaxation times (or equivalently β_{KWW}) is temperature invariant, the changes in T reduce to a rescaling of the time axis such that shifting the curves along the $\log(t)$ scale allows the data to form a master curve. This time–temperature superposition principle bears no general validity but holds for a number of polymers in a limited temperature interval[9].

The characteristic or average time scale $\langle\tau\rangle$ of the dynamics are often found to follow a Vogel–Fulcher–Tammann[10,11] (VFT) like variation with temperature, according to

$$\langle\tau\rangle = A \exp[B/(T - T_0)] \quad (2)$$

An extrapolation of the VFT law towards temperatures below those where the relaxation time is experimentally accessible implies a practically frozen structure already at $T \approx T_g - 20\,K$. Since the observed VFT dependence refers to equilibrium relaxation data, such an extrapolation towards $T \ll T_g$ is valid only for systems which remained in thermodynamic equilibrium during the entire cooling process from the supercooled liquid to the frozen 'glassy' state. At practical cooling rates, however, the system will depart from the equilibrium behaviour near T_g^* to become arrested in a metastable state which is often described by a fictive temperature T_f which tends to relax towards the actual sample temperature T[4]. The basis for $T_f \neq T$ is that the thermal history has not given the system sufficient time to relax its volume or density entirely.

Among the various methods used to study the relaxational behaviour of soft condensed matter, dielectric relaxation techniques yielding $\epsilon^*(\omega)$ or $\epsilon(t)$ offer a

*To whom correspondence should be addressed

straightforward access to the molecular dynamics over a large range of time scales[12,13]. The slow processes occurring near or below the calorimetric T_g^* are often investigated by isothermal time domain techniques[12,14] or thermally activated depolarization current measurements[15–20], where in both cases the current $I(t)$ or charge $Q(t)$ is measured under the condition of a constant electric field $E = E_0$ and the polarization is given by $P(t) \propto D(t) = Q(t)/A \propto \int I(t)\mathrm{d}t$. In a recent paper[5] we have measured the dielectric modulus $M(t)$ in isothermal experiments in the time range 10^{-3}–10^6 s. The modulus has been recorded by measuring the electric field $E(t)$ of the sample capacitor under the condition of a constant dielectric displacement $D = D_0$, so that $M(t)$ and $E(t)$ are proportional to the polarization $P(t)$[12]. In the frequency domain the relation between the retardation $\epsilon^*(\omega)$ and relaxation $M^*(\omega)$ is simply $M^*(\omega) = 1/\epsilon^*(\omega)$[21]. Although the two quantities both reflect orientational polarization of permanent dipoles, their characteristic time scales $\langle\tau\rangle$ as well as the corresponding distributions of τ can differ significantly. For the Debye case of a single relaxation time the relation between the constant field (τ_ϵ) and constant displacement (τ_M) time constants can be obtained from a straightforward calculation and reads $\tau_M = \tau_\epsilon \cdot \epsilon_\infty/\epsilon_s$, where ϵ_∞ and ϵ_s denote the dielectric constants in the limit of high and low frequencies, respectively[12,22]. For materials subject to a broad distribution of relaxation times, the relation between $\langle\tau_M\rangle$ and $\langle\tau_\epsilon\rangle$ has to be evaluated numerically with the result that the ratio $\langle\tau_M\rangle/\langle\tau_\epsilon\rangle$ attains values significantly below $\epsilon_\infty/\epsilon_s$[23]. Because $M(t)$ decays faster than the dielectric function $\epsilon(t)$, this technique allowed for measuring average dielectric time constants τ_ϵ between 10^{-2} s and 10^7 s, which corresponds to dynamics which are roughly up to five decades slower than those at the calorimetric glass transition with $\tau_\epsilon \approx 100$ s[5].

The scope of the present work is twofold. One aspect is to present a novel method of detecting thermally stimulated relaxation processes in terms of modulus measurements $M(T,t)$, in the following termed TSMR for thermally stimulated modulus relaxation. The technique is to cool the unpoled sample in disc capacitor geometry to well below T_g, charging this capacitor to a practical voltage, and then monitoring the decay of the voltage $U(t) \propto E(t)$ while ramping the temperature. The second aspect is to present a straightforward method of data analysis with only the common prerequisite of the knowledge of the distribution of relaxation times whose form is assumed temperature invariant. Without a data fitting procedure, the proposed algorithm directly translates the $M(T,t)$ data into a temperature dependent characteristic time constant. The results are then compared to the isothermal data for the equilibrated sample obtained under otherwise identical conditions.

EXPERIMENTAL

Poly(vinylacetate) with a viscosimetric average molecular weight of $M_w = 14000$ and a dispersity of 3 was obtained from Wacker, Germany. The PVAc material has been recrystallized and dried under vacuum for 3 days. D.s.c. determined the calorimetric glass transition temperature extrapolated to zero heating rate to be $T_g^* = 299.6$ K. Preparing the capacitor is achieved by melting PVAc on a 40 mm ∅ gold plated brass disc and covering the sample by a second 20 mm ∅ plate. The plate separation has been defined by 50 μm Teflon-spacers of negligible area relative to the capacitor discs. The sample capacitor was temperature controlled by a N_2 gas flow emerging from a l-N_2 dewar which could be appropriately heated prior to passing the sample. For measuring the sample temperature we employed a Pt-100 sensor mounted inside the larger brass plate of the capacitor.

At $t = 0$ the capacitor is charged to a voltage of ≈ 30 V within 10 μs and then insulated entirely from the charging circuit supplied by the voltage source of the electrometer. The connection between sample and electrometer Keithley 6517 ($R_i > 200$ TΩ) consists of a coaxial air line with $C \approx 15$ pF inside the cryostat and a 50 cm low-noise triax cable between cryostat and electrometer input.

The procedure of the temperature ramping experiment is as follows. Sample, experimental setup, and charging voltage for the TSMR run were identical to the isothermal cases reported previously[5]. The PVAc has been equilibrated well above its T_g^* and cooled at a rate of 5 K min^{-1} to the start temperature of 0°C *without* application of an electric field. At $T = 0$°C (and $t = 0$) the capacitor is charged, the temperature is increased at a rate of ≈ 20 mK s^{-1} = 1.2 K min^{-1}, and both temperature and voltage across the capacitor are recorded as a function of time in steps of 3.6 s.

RESULTS

In *Figure 1* we show the temporal evolution of the temperature in course of the TSMR experiment. As will be discussed below the data analysis is not bounded to a linear ramp as long as $T(t)$ is known. The resulting TSMR trace $M(T,t)$ in the range 0°C to 50°C normalized to $M_\infty = \epsilon_\infty^{-1}$ is displayed in *Figure 2*, which also includes the derivative $\partial M(T,t)/\partial t$ as a dashed curve. The value for $\partial M(T,t)/\partial t$ at time t_i is obtained without any smoothing procedures using $[M(T,t_{i+1}) - M(T,t_{i-1})]/[t_{i+1} - t_{i-1}]$, where t_{i-1}, t_i, and t_{i+1} are three successive data points from the $M(T,t)$ curve. Both curves in *Figure 2* are shown with their entire experimental noise, i.e. without smoothing or fitting. As obvious from the isothermal results[5] the features below 305 K reflect the structural α-process of PVAc, whereas at higher temperatures $M(T,t)$ is governed by d.c.-conductivity.

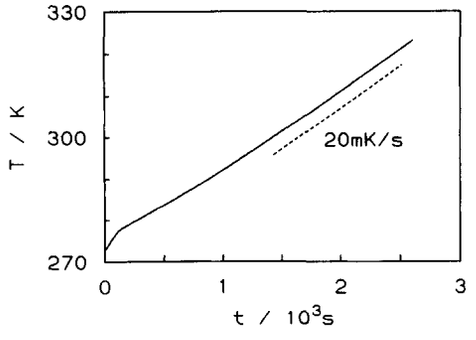

Figure 1 Sample temperature vs. time during the TSMR $T(t)$ ramp (solid line). The dashed line indicates the average heating rate of 20 mK s^{-1} or 1.2 K min^{-1}. Note that the data analysis is not restricted to a linear T–t relation

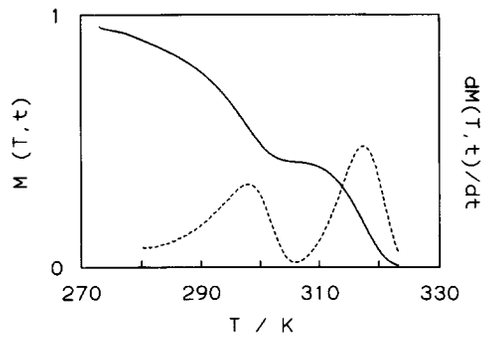

Figure 2 Temperature (and implicitly time) dependence of the voltage $U(T,t)$ across the sample capacitor at constant dielectric displacement D_0 in course of the TSMR experiment on PVAc using the temperature ramp of *Figure 1*. The solid line plots the results in terms of the modulus $M(T,t)$ [$\propto U(T,t)$] normalized to M_∞. The dashed line shows $\partial M(T,t)/\partial t$ in arbitrary units with the α-peak at $T \approx 298$ K and the ρ-peak at $T \approx 317$ K

The isothermal results in the range $291\,\mathrm{K} \leq T \leq 323\,\mathrm{K}$ obtained previously[5] for this sample can be summarized as follows. Including the conductivity contribution with time constant $\tau_\sigma = \sigma_{dc}^{-1} M_s^{-1} \epsilon_0$, the entire $M(t)/M_\infty$ curves are well represented by a KWW type structural relaxation and an exponential conductivity term

$$M(t) = (M_\infty - M_s)\exp[-(t/\tau_{KWW})^{\beta_{KWW}}] + M_s \exp[-t\sigma_{dc} M_s \epsilon_0^{-1}], \quad (3)$$

where $M_\infty = \epsilon_\infty^{-1}$ and $M_s = \epsilon_s^{-1}$ denote the dielectric modulus in the limits $t \to \infty$ and $t \to 0$, respectively, regarding only the orientational polarization effects, i.e. for $\sigma_{dc} = 0$. The relaxation time τ_{KWW} follows a VFT type temperature dependence [equation (2)] with the parameters $\log_{10}(A) = 11.4$, $B = 1184$ K and $T_0 = 261$ K. The dispersion parameter β_{KWW} is 0.40 ± 0.02 with a slightly systematic variation with temperature as low as $d\beta_{KWW}/dT \leq 10^{-3}\,\mathrm{K}^{-1}$ according to linear regression, i.e. $\beta_{KWW} \neq \beta_{KWW}(T)$. Since this result for β_{KWW} implies a temperature independant form of the distribution of relaxation times, the time–temperature superposition principle holds for PVAc in this experimental temperature range to a good approximation.

DATA ANALYSIS

In standard measurements of thermally stimulated depolarization (TSD) measurements one records the current $I(T,t)$ at constant field $E = 0$ after preparing an electret at temperatures well below T_g[15,20]. The resulting $I(T,t)$ trace relates to the derivative $\partial P/\partial t$ of the polarization and displays a peak at temperatures where some motion of charge is active on a time scale set by the heating rate[15]. It is only for the sake of a rough comparison that we show in *Figure 2* the derivative $\partial M(T,t)/\partial t$, which is therefore similar to TSD curves[19]. It should be emphasized, however, that the polarizations $P(T,t)$ measured under constant field (TSD) and constant displacement (TSMR) conditions are not related in a trivial manner.

The interpretation of TSD results has been addressed frequently[15–20,24,25] and in practically all cases it seems impossible to unambiguously extract both the distribution of relaxation times and the temperature dependence from a single TSD run[26]. The common requirement for a reasonable data analysis is the knowledge of the distribution $G(\tau)$ of retardation or relaxation times whose functional form is assumed to be temperature invariant. For PVAc in the temperature range of interest, this condition is fulfilled according to the isothermal results. In terms of the probability density $g(\tau) = dG(\tau)/d\tau$ the orientational polarizability contribution to the modulus at constant temperature T_0 reads

$$M(T_0,t) = M_s + (M_\infty - M_s)\int_0^\infty g(x)e^{-t/x\tau(T_0)}dx \quad (4)$$

where $g(x)$ is normalized such that $\int_0^\infty g(x)dx = G(\infty) = 1$, $G(\tau)$ being the distribution function. Instead of using $g(\tau)$, we introduce $g(x)$ such that x reflects a dimensionless scaling parameter for τ (appearing as $x \cdot \tau$), so that $g(x)$ will not shift with τ or T. In this notation, $g(x)$ is independent of temperature and the variation of the average relaxation time scale with temperature is completely cast into $\tau(T)$. Following common practice the temperature dependences of M_s and M_∞ are also assumed negligible. Instead of the numerically difficult probability density $g_{KWW}(x)$[27] related to a KWW type decay, we prefer employing the more practical function $g_{HN}(x)$ related to the commonly used dielectric function $\epsilon^*(\omega)$ of the Havriliak–Negami[28] (HN) type given by

$$\epsilon^*(\omega) = \epsilon_\infty + (\epsilon_s - \epsilon_\infty)[1 + (i\omega\tau_{HN})^{\alpha_{HN}}]^{-\gamma_{HN}} \quad (5)$$

In equation (5) the shape parameters α_{HN} and γ_{HN} in the limits $0 < \alpha_{HN}$, $\alpha_{HN}\gamma_{HN} \leq 1$ characterize the symmetric and asymmetric broadening of the dielectric loss, respectively, while $\alpha_{HN} = \gamma_{HN} = 1$ restores the case equivalent to a single exponential decay in the time domain. The probability density for τ leading to the form of equation (5) takes the form[29]

$$g_{HN}(\tau) = \frac{(\tau/\tau_{HN})^{\alpha\gamma}\sin(\gamma\Phi)}{\pi\tau[(\tau/\tau_{HN})^{2\alpha} + 2(\tau/\tau_{HN})^{\alpha}\cos(\pi\alpha) + 1]^{\gamma/2}} \quad (6)$$

with

$$\Phi = \arctan\frac{\sin(\pi\alpha)}{(\tau/\tau_{HN})^{\alpha} + \cos(\pi\alpha)}$$

The values $\alpha_{HN} = 0.8$ and $\gamma_{HN} = 0.4$ inserted in equation (6) yield a density $g_{HN}(\tau)$ which resembles $g_{KWW}(\tau)$ for $\beta_{KWW} = 0.40$ with a sufficient degree of accuracy for the present purpose. Therefore we employ $g_{HN}(\tau)$ with $\alpha_{HN} = 0.8$, $\gamma_{HN} = 0.4$, and $\tau_{HN} = 1$ as $g(x)$ in equation (4) so that $M(t) \propto \exp[-(t/\tau)^{0.4}]$ would result for a constant temperature. The above special case for $g(\tau)$ is depicted as a solid line in *Figure 3* in terms of the probability density $\tau g(\tau)$ vs. $\ln(\tau)$. Consider now an isothermal relaxation subject to the above distribution of τ, which reflects the picture of parallel first order reactions with rate constants $1/\tau$ occurring with probabilities as shown in *Figure 3*. The ensemble averaged decay is non-exponential because sites with small τ will govern the short time response, whereas the density at larger τ will become effective at longer times. In the following, the integrand in equation (4), $g(\tau)\exp(-t/\tau)$, shall be denoted $g_{occ}(\tau,t)$ which can be interpreted as the probability density of those sites which have not yet contributed to the decay at time t, i.e. the remaining occupation of $g(\tau)$ as a function of time. The evolution of $g_{occ}(\tau,t)$ is also shown in *Figure 3* as dashed

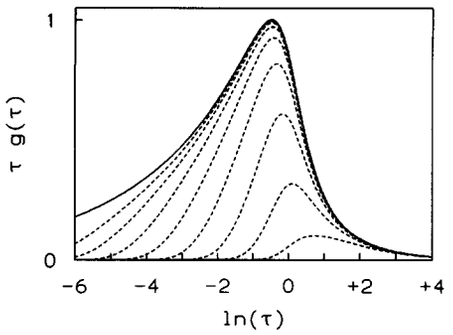

Figure 3 The solid line plots the probability density $h_{HN}(\ln\tau) = \tau g_{HN}(\tau)$ (normalized to its peak value) according to equation (6) for the parameters $\alpha_{HN} = 0.8$, $\gamma_{HN} = 0.4$ and $\tau_{HN} = 1$. The dashed lines plot $\tau g_{occ}(\tau, t) = \tau g(\tau)\exp(-t/\tau)$ for times $\ln(t) = -6 \ldots +1$ in steps of 1 and in the order from top to bottom curve. The function $g_{occ}(\tau, t)$ corresponds to the probability density of sites or 'relaxors' which are not yet equilibrated at time t

lines for a series of logarithmically spaced times. The slowing down of a KWW type decay relative to the initial exponential decrease can thus be viewed as a consequence of $g_{occ}(\tau, t)$ shifting towards larger values of τ as time proceeds.

For analysing the TSMR trace $M(T, t)$ along the above lines it suffices to find the appropriate $\tau(t)$ such that

$$\frac{\partial M(T,t)}{\partial t} = -\frac{1}{\tau(t)}\int_0^\infty x^{-1} g_{occ}(x,t)\mathrm{d}x\, M(T,t) \qquad (7)$$

with

$$\frac{\partial g_{occ}(x,t)}{\partial t} = -\frac{1}{x\tau(t)} g_{occ}(x,t) \quad \text{and} \quad g_{occ}(x,0) = g(x)$$

The basis for equation (7) is that at a given time t' the system memorizes its kinetic history for $t < t'$ only by means of the evolution of $g_{occ}(x, t)$ as defined above and sketched in *Figure 3*. Solving for $\tau(t)$ in equation (7) at given $g(x)$ and $M(T, t)$ reduces to a straightforward procedure if one recalls that for a decay with arbitrary $g(\tau)$ one has

$$\phi(t) = \int_0^\infty g(\tau)\, \mathrm{e}^{-t/\tau}\mathrm{d}\tau \quad \Rightarrow \quad \left.\frac{\mathrm{d}\phi(t)}{\mathrm{d}t}\right|_{t=0} = -\langle 1/\tau\rangle \qquad (8)$$

A practical numerical route for evaluating equation (7) is as follows. At time t_0 one has to set

$$\tau(t_0) = -\int x^{-1} g_{occ}(x, t_0)\, \mathrm{d}x\, M(T, t_0)\Delta t / [M(T, t_0 + \Delta t) - M(T, t_0)]$$

where the integral represents the average $\langle 1/x\rangle$ of the current occupational density $g_{occ}(x, t_0)$. With this $\tau(t_0)$ one calculates $g_{occ}(x, t_0 + \Delta t)$ according to equation (7), repeats the first step at $t_0 + \Delta t$, and so on. For sufficiently small Δt one obtains $\tau(t)$ such that equation (7) reproduces the $M(T, t)$ data within any desired accuracy. Note that the temporal evolution of the temperature $T(t)$ can be ignored up to this stage. Since τ has been introduced such that it contains no explicit dependence on time, we use $T(t)$ to translate $\tau(t)$ into $\tau(T)$, which now indicates how temperature shifts the probability density $g(\tau)$ on the $\ln(\tau)$ scale.

Analytically or numerically, the above procedure outlined by equation (7) and below can be shown to yield the identical result as the standard formulation,

$$M(T,t) = M_s + (M_\infty - M_s) \times \int_0^\infty g(x)\exp\left(-\int_0^t 1/x\tau(t')\mathrm{d}t'\right)\mathrm{d}x \qquad (9)$$

used for expressing $M(T, t)$ in terms of $g(x)$ and $\tau(T)$. However, because equation (9) does not serve as a straightforward recipe for deriving $\tau(T)$, this formulation is useful only for a fit routine which optimizes $\tau(T)$ such that $M(T, t)$ is recovered at a given probability density of relaxation times.

The TSMR data shown in *Figure 2* have been analysed along the above lines. In addition, however, a δ-like peak with relative weight $M_s/M_\infty = 0.436$ is added to the probability density $g(\tau)$ at $\ln(\tau_\sigma) = +9.6$ in order to account for the contribution of d.c.-conductivity[30]. In *Figure 2* the initial decay of the level of M_s/M_∞ is due to the structural relaxation (α-peak), the remaining decrease stems from the ohmic conductivity (σ_{dc}) which leads to an exponential decay in an isothermal $M(t)$ experiment (ρ-peak)[15–20]. Both values, τ_σ and M_s/M_∞ are known from the isothermal data, so that the calculation for $\tau(T)$ involves no free parameter. The result for $\tau(T)$ inferred from the data of *Figure 2* is outlined as a dashed line in *Figure 4*, which also compares this $\tau(T)$ from the TSMR experiment to the isothermal equilibrium data. The deviations between $\tau(T)$ and the equilibrium data above $T = 306$ K arise because d.c.-conductivity and α-process are subject to slightly different temperature dependences, which has been ignored in the above calculation. Because the HN-probability density $g_{HN}(\tau)$ has been used with $\tau_{HN} \equiv 1$, the $\tau(T)$ result actually refers to $\tau_{HN}(T)$ so that the isothermal τ-data in *Figure 4* are scaled accordingly.

DISCUSSION

A time domain measurement of the dielectric modulus is a conceptually simple method for detecting dielectric relaxations, the only critical experimental requirement being the high impedance of the voltmeter if time scales of $> 10^6$ s are to be addressed. In the TSMR experiment described above typical acquisition times are some 10^3 s, so that standard devices with 1 TΩ input and 10 V voltage range are sufficient in this case. As the starting temperature T_0 is usually selected to assume a negligible

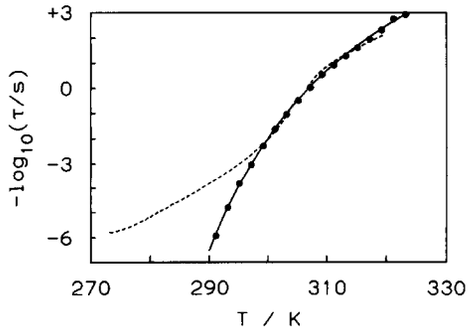

Figure 4 Temperature dependence of the characterstic relaxation times τ_{HN} from modulus measurements on PVAc. Dots refer to isothermal equilibrium measurements from previous work[5]. The solid line is a VFT fit to the isothermal data. The dashed line is the $\tau(T)$ result from the TSMR experiment obtained according to the procedure described in the text [see equation (7) and below] with no free parameter

decay at $T = T_0$, charging the capacitor via a relay within ~ 10 ms to $U_0 = 10$ V is sufficiently fast for a TSMR experiment. For low loss materials the voltmeter should resolve the range U_0 to $U_\infty = \epsilon_\infty/\epsilon_s\, U_0$, where U_∞ is the plateau voltage before d.c.-conductivity forces $U(t)$ to zero. We emphasize again that the pattern of polarization or depolarization is not a material specific quantity alone, but also depends on the experimental situation, constant displacement D_0 or constant field E_0[21,22]. Equivalently, for a comparison of modulus results $M(t)$ to standard dielectric data $\epsilon(t)$ it should be kept in mind that $M(t)$ decays faster by at least a factor of $\epsilon_s/\epsilon_\infty$ relative to $\epsilon(t)$ as inferred from conventional time domain dielectric techniques at constant field.

For practical purposes, the TSMR technique presented here bears the advantage of having to detect only moderate voltages after cooling the sample at zero field. Instead, the TSD method either yields very small currents or the sample must be polarized above T_g with sufficiently high electric fields. In addition, the direct evaluation of $M(T,t) \rightarrow \tau(T)$ at a certain temperature T_a uses the data for $T \leq T_a$ only, so that a real time display of $\tau(T)$ in the course of the TSMR run is possible. For the material science this resembles an effective tool for characterizing the molecular dynamics in the glassy state of matter as a function of thermal treatment or annealing.

The direct numerical analysis outlined above is of course not restricted to the TSMR technique, but can equally be applied to the polarization changes $D(t)$ from TSD experiments. Assuming the knowledge and temperature-invariance of the relaxation or retardation time distribution, casting the $P(T,t)$ data into a $\tau(T)$ representation in the above manner can be considered exact and does not require assumptions about the functional dependence of $\tau(T)$ nor does it involve fit procedures.

The observation in *Figure 4* of a significant and systematic deviation between equilibrium and thermally stimulated or non-equilibrium data is a common feature[31] and can be rationalized by straightforward arguments. At the calorimetric glass transition $T_g^* = 299.6$ K the average equilibration time is several minutes, so that cooling the sample at a rate of $\approx 5\,\mathrm{K\,min^{-1}}$ must result in a departure from thermodynamic equilibrium at temperatures near 300 K for PVAc. Therefore, critical properties like free volume, density, or configurational entropy become arrested at values related to temperatures T_f in excess of the actual sample temperature T upon preparing the initial state at $T_0 \ll T_g^*$. Thereby, T_f naturally depends on the thermal history of the sample. If the dielectric relaxation time $\tau(T)$ is taken as a measure for the fictive temperature, T_f has not attained values below ~ 290 K, although the TSMR run started at $T_0 = 273$ K. Therefore, without having to extrapolate the measurement VFT-like equilibrium data $\tau_{eq}(T)$ we can obtain $T_f(T)$ as shown in *Figure 5* via $\tau(T_f) = \tau_{eq}(T)$, where $\tau(T_f)$ refers to the TSMR result.

A more quantitative approach to such a relaxation time scenario has been given by Adam and Gibbs[32] on the basis of 'cooperatively rearranging regions' subject to a temperature dependent spatial extent. The resulting relaxation time τ as a function of configurational entropy $S_c = S_c(T)$ takes the form

$$\tau = \tau_0 \exp[C/TS_c] \qquad (10)$$

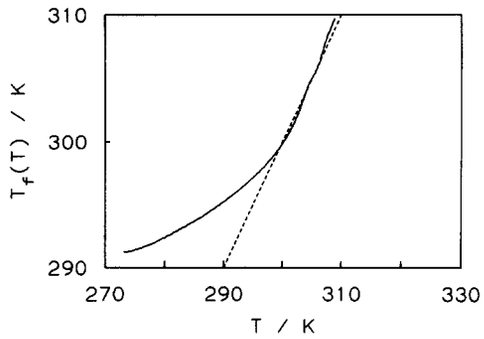

Figure 5 Fictive temperature $T_f(T)$ vs. sample temperature T as obtained from the TSMR data for PVAc on the basis of $\tau(T_f) = \tau_{eq}(T)$ where τ and τ_{eq} refer to the thermally stimulated and equilibrium isothermal data, respectively. Note that no extrapolation of $\tau_{eq}(T)$ beyond the experimental temperature range is involved

with

$$S_c = \begin{cases} \kappa(T - T_\infty)/T, & T \geq T_g \quad \text{[equilibrium} \\ & \qquad\qquad S_c = S_c(T)\text{]} \\ S_c(T_g) & T \leq T_g \quad \text{(frozen } S_c = \text{constant)} \end{cases}$$

where in the equilibrium case $(T \geq T_g)S_c$ is assumed to decrease linearly with T such that it vanishes at a finite temperature T_∞. For temperatures $T > T_g$ the $\tau(T)$ curve expected on the basis of equation (10) displays a Vogel–Fulcher–Tammann type of behaviour, $\tau = \tau_0 \exp[C/\kappa(T - T_\infty)]$. Below T_g the configurational entropy (but not the relaxation itself) becomes frozen at its value $S_c(T_g)$, i.e. S_c no longer depends on T in this range, with the consequence that $\tau(T)$ in equation (10) merges into an Arrhenius like temperature dependence $\tau = \tau_0 \exp[C/TS_c(T_g)]$. At least qualitatively, such a model conforms well with the observed features compiled in *Figure 4*. The difference between the isothermal and thermally stimulated $\tau(T)$ also emerges naturally from the above picture: in the TSMR experiment the cooling and heating rates are of the order of the rates used in the calorimetric determination of the glass transition temperature $T_g^* = 299.6$ K for PVAc. Under the experimental condition yielding the isothermal equilibrium data the glass transition has been shifted to $T_g \leq 291$ K. The latter case thus results in a VFT like temperature dependence of the relaxation time over the entire experimental range. The former case, however, displays a more Arrhenius like behaviour for $T < T_g^*$ and merges into the VFT curve for higher temperatures $T > T_g^*$, where the system is capable of equilibrating sufficiently fast.

From the above understanding of the TSMR results it follows that only little can be learned about the equilibrium dynamics if cooling rates around several $\mathrm{K\,min^{-1}}$ are used in preparing the thermally stimulated experiment. Note that the α-process contribution to $M(T,t)$ has relaxed almost entirely in the temperature range $T < T_g^*$ where non-equilibrium conditions prevail. In order to retrieve the equilibrium data shown for $T \geq 291$ K from a single TSMR run an extremely slow cooling rate is necessary such that preparing the initial electret would involve several 10^6 s, i.e. the same time is needed to have equilibrated the sample prior to taking the isothermal data point at 291 K. Consequently, the formation of a glassy state at practical cooling rates will by no means lead to properties expected on the

basis of extrapolating equilibrium data towards lower temperatures.

ACKNOWLEDGEMENTS

We thank D. Neher and F. Stickel for stimulating discussions. Financial support by the Fonds der Chemischen Industrie is gratefully acknowledged.

REFERENCES

1. Donth, E., *Relaxation and Thermodynamics in Polymers*. Akademie Verlag, Berlin, 1992.
2. Winkelhahn, H.-J., Servay, Th. K. and Neher, D., *Ber. Bunsenges. Phys. Chem.*, 1996, **100**, 123.
3. Schüssler, S., Richert, R. and Bässler, H., *Macromolecules*, 1995, **28**, 2429.
4. Jäckle, J., *Rep, Prog. Phys.*, 1986, **49**, 171.
5. Wagner, H. and Richert, R., *Polymer*, 1997, **38**, 255.
6. Richert, R. and Blumen, A. (eds), *Disorder Effects on Relaxational Processes*. Springer, Berlin, 1994.
7. Kohlrausch, R., *Pogg, Ann. Phys.*, 1854, **91**, 179.
8. Williams, G. and Watts, D. C., *Trans. Faraday Soc.*, 1970, **66**, 80.
9. Ferry, J. D., *Viscoelastic Properties of Polymers*, 3rd edn. Wiley, New York, 1980.
10. Vogel, H., *Phys. Z.*, 1921, **22**, 645.
11. Fulcher, G. S., *J. Am. Ceram. Soc.*, 1923, **8**, 339.
12. McCrum, N. G., Read, B. E. and Williams, G., *Anelastic and Dielectric Effects in Polymeric Solids*. Dover, New York, 1991.
13. Stickel, F., Fischer, E. W. and Richert, R., *J. Chem. Phys.*, 1995, **102**, 6251; 1996, **104**, 2043.
14. Mopsik, F. I., *Rev. Sci. Instrum.*, 1984, **55**, 79.
15. Van Turnhout, J., *Thermally Stimulated Discharge of Polymer Electrets*. Elsevier, Amsterdam, 1975.
16. Van Turnhout, J., in *Topics in Applied Physics 33: Electrets*, Chapter 3, ed. G. M. Sessler. Springer, Heidelberg, 1987.
17. Bucci, C. and Fieschi, R., *Phys. Rev. Lett.*, 1964, **12**, 16.
18. Gross, B., *Charge Storage in Solid Dielectrics*. Elsevier, Amsterdam, 1964.
19. Lacabanne, C. and Chatain, D., *J. Polym. Sci. Polym. Phys.*, 1973, **11**, 2315.
20. Vanderschueren, J. and Gasiot, J., in *Topics in Applied Physics 37: Thermally Stimulated Relaxation in Solids*, Chapter 4, ed. P. Bräunlich. Springer, Heidelberg, 1975.
21. Gross, B., *Kolloid Z.*, 1953, **131**, 168; **134**, 65.
22. Fröhlich, H., *Theory of Dielectrics*. Clarendon, Oxford, 1958, p. 72.
23. Richert, R. and Wagner, H., *J. Phys. Chem.*, 1995, **99**, 10948.
24. Winkelhahn, H.-J., Schrader, S., Neher, D. and Wegner, G., *Macromolecules*, 1995, **28**, 2882.
25. Halpern, V., *J. Phys. D*, 1993, **26**, 307.
26. Böttcher, C. J. F. and Bordewijk, P., *Theory of Electric Polarization*, Vol. 2. Elsevier, Amsterdam, 1978.
27. Linsey, C. P. and Patterson, G. D., *J. Chem. Phys.*, 1980, **73**, 3348.
28. Havriliak, S. and Negami, S., *J. Polym. Sci. Polym. Symp.*, 1966, **14**, 89.
29. Havriliak, S. and Negami, S., *Polymer*, 1967, **8**, 161.
30. Macedo, P. B., Moynihan, C. T. and Bose, R., *Phys. Chem. Glasses*, 1972, **13**, 171.
31. Alegría, A., Guerrica-Echevarría, E., Goitiandía, L., Tellería, I. and Colmenero, J., *Macromolecules*, 1995, **28**, 1516.
32. Adam, G. and Gibbs, J. H., *J. Chem. Phys.*, 1965, **43**, 139.